

REVIEWS OF TOPICAL PROBLEMS

PACS numbers: 07.07.Df, 37.10.De, 37.10.Gh

55th ANNIVERSARY OF THE INSTITUTE OF SPECTROSCOPY
OF THE RUSSIAN ACADEMY OF SCIENCES (ISAN)

Atom chip

A E Afanasiev, P I Skakunenko, D V Bykova, A S Kalmykov, V I Balykin

DOI: https://doi.org/10.3367/UFNe.2024.09.039752

Contents

Abstract. The first atom chip in Russia — a device for cooling, trapping, and controlling neutral atoms — was created at the Institute of Spectroscopy, Russian Academy of Sciences. Atom chips are a platform for creating quantum sensors based on ultracold atoms. Atom chip technology underlies experiments with atoms in the state of Bose–Einstein condensation currently being conducted aboard the International Space Station. Progress in this area will allow creating atomic clocks, gravimeters, and inertial sensors that can be used in both fundamental and applied problems.

Keywords: atom chips, quantum sensors, laser cooling of atoms, atom traps

1. Introduction

Atomic quantum sensors (QSs) [1] have attracted considerable attention over the last few decades due to spectacular progress in laser cooling and trapping of atoms [2–4]. Using laser cooling, important results have been obtained in fundamental physics, including the state of Bose–Einstein condensation [5] and Fermi gases [6, 7], and methods for their control have been developed [8, 9]. From a practical standpoint, keen interest in laser cooling is associated with the creation of highly stable clocks [10, 11].

Currently, the range of applications of cold atoms is expanding, in particular, to the construction of quantum computers [12], simulators [13, 14], and sensors [1]. Sensors based on cold atoms can be created using various approaches. Cold atom QSs can be conventionally divided into two large groups: those reliant on interference effects and those not reliant on them. The latter group includes, for example, vacuum gauges [15–17], gravimeters based on optical clocks [18, 19], and electromagnetic field sensors. The use of cold atoms in such sensors ensures the required level of sensitivity. For example, a gravimeter based on cold atoms can be built based on an optical frequency standard. According to the general theory of relativity, the frequency of the atomic standard depends on the gravitational potential at the location of the clock. Measuring the difference in the rate of two clocks spaced apart allows measuring the difference in the gravitational potential [20] and hence the relative acceleration of gravity. The accuracy of the measurement depends on the stability of the atomic clock, which now reaches 10^{-18} for optical frequency standards that do not use interference methods [10]. The choice of an atomic clock as a QS will allow searching for the drift of fundamental constants [21].

One of the most common approaches to constructing QSs is the use of coherent effects in a quantum system [22], which allows creating interferometers and thereby increasing the sensitivity. The operation of a QS is then based on measuring the phase difference between two quantum paths that occur due to some interaction. This principle underlies the operation of gravimeters [23–28], gradiometers [29, 30], gyroscopes [31–34], and accelerometers [35]. Microwave atomic clocks, which are used to define the second in the SI system, are also an example of an interferometry-based QS.

A E Afanasiev [(1,2,a)], **P I Skakunenko** [(1,b)], **D V Bykova** [(1,2,c)], **A S Kalmykov** [(1,d)], **V I Balykin** [(1,e)]
[(1)] Institute of Spectroscopy, Russian Academy of Sciences, ul. Fizicheskaya 5, 108840 Troitsk, Moscow, Russian Federation
[(2)] National Research University Higher School of Economics (HSE University), ul. Myasnitskaya 20, 101000 Moscow, Russian Federation
E-mail: [(a)] afanasiev@isan.troitsk.ru, [(b)] skakunenko.pi@phystech.edu, [(c)] bykova.darya2000@gmail.com, [(d)] kalmykov_100@mail.ru, [(e)] balykin@isan.troitsk.ru

Received 12 March 2024, revised 3 September 2024
Uspekhi Fizicheskikh Nauk **194** (11) 1146 – 1158 (2024)
Translated by S Alekseev

In atomic interferometers that use cold atoms, the operation of the QS consists of several stages: preparation of a cloud of ultracold atoms, preparation of the interferometer, and measurement of the interference pattern. At the initial preparation stage, the atoms are cooled by laser radiation and trapping so as to make up a point source. The temperature of the atoms determines the possible time of transit trough the atomic interferometer. This time is limited by the expansion of the atomic ensemble due to a finite temperature. In some atomic interferometers, evaporative cooling is used to achieve ultralow temperatures and, if necessary, the state of Bose–Einstein condensation. The freely falling cloud of cold atoms in a QS undergoes a wave of coherent splitting and recombination involving lasers. Finally, the output quantum state of an atom (already dependent on the external measurable factors) is measured, typically using fluorescence or absorption visualization. The ultimate sensitivity of an atomic QS is determined by two main physical parameters: 1) the time of transit T of atoms through the atomic interferometer and 2) the number of atoms N in the ultracold cloud. On Earth, the time of transit of atoms through a compact QS is limited to fractions of a second by the possible vacuum chamber size. In some setups, this time can be increased to 2 s by increasing the setup size to 10 m. In space, because the sensitivity of the QS scales with the time of transit as $2T$, QSs significantly gain in sensitivity due to the long 'free-fall' time of atoms in microgravity conditions. The second factor limiting the sensitivity of a QS is the number of atoms N in the ultracold cloud. Increasing the number of atoms by a factor of N allows increasing the sensitivity by a factor of $\sqrt{N}$. This limitation is known as the standard quantum limit.

There is also another fundamental and technological factor limiting the use of QSs. Currently, both on Earth (outside laboratory conditions) and in space, the following requirements are put forward for QSs: minimization of size (S), weight (W), and power (P) consumption — the so-called SWaP criteria. Meeting at least one of these criteria is sufficient grounds for the practical use of a QS outside the laboratory; meeting all three criteria is a fundamentally necessary condition for the successful use in space.

A solution that satisfies the SWaP criteria in an atomic QS is the use of atom chip technology. The basic concept of an atom chip is a simple configuration of magnetic and laser fields that allows cooling and trapping atoms and controlling their internal and external degrees of freedom [36]. The simplest scheme of an atom chip is a microwire (straight or bended) carrying electric current, manufactured using nanolithography methods on the surface of a dielectric, and an external uniform magnetic field. The surface reflects the laser light, with a six-beam configuration arranged near the surface to make up a magneto-optical trap (MOT) for the primary stage of cooling the atoms.

The atom chip concept combines advanced semiconductor industry technologies and achievements in atomic optics to create a 'solid-state' device (chip) for atomic optics (analogous to an electronic chip). This approach makes it possible to ensure, on the one hand, precision, scalability, miniaturization, and integration thanks to semiconductor industry technologies, and, on the other hand, a long coherence time of isolated ultracold atomic matter. There has been and still is hope that this level of miniaturization and integration would bring about a revolution in atomic optics like the one it has already brought to electronics and optics.

2. Atom chip as a source of atoms for quantum sensors

To create atomic QSs, an atom ensemble must be formed. There are four main approaches to the formation of atom sources (Fig. 1): (a) atomic vapor cell; (b) atomic beams; (c) a three-dimensional MOT of atoms; and (d) atoms trapped in the vicinity of an atom chip.

The use of atomic vapor cells is one of the simplest ways to form an atom system for constructing QSs. An example of the use of this approach is given by atomic vapor cells in magnetometers [37, 38] and compact atomic clocks [39, 40]. The accuracy of sensors based on atomic vapor cells is largely limited by the thermal motion of atoms. An ensemble of cold atoms can be formed in such systems, but the coherence time is limited by the interaction of cold atoms and residual thermal atoms.

Atomic beams are one of the most effective sources of atoms in quantum sensoring. The effects of atomic diffraction on slit nanostructures have been demonstrated with thermal atomic beams [41]. Using two-dimensional laser cooling (optical molasses) [42, 43] for an atomic beam, a high degree of its monochromatization in the transverse direction can be achieved. Monochromatization in the longitudinal direction is possible using ultrasonic nozzles [44]. An outstanding example of the use of an atomic beam for quantum sensoring was demonstrated by Prof. Kazevich's group. Based on the method of atomic interferometry, they created a Sagnac interferometer for detecting rotation [45]. Due to the large area of the interferometer, they could achieve record values of sensitivity to rotation, at the level of 6×10^{-10} rad s^{-1} at integral times of 1 s [46].

An important advantage of atomic interferometers with an atomic beam as a source of atoms is the possibility of continuous measurement, which significantly increases the accuracy of such a sensor compared to others, where the preparation of the atomic ensemble, its evolution in the interferometer, and subsequent reading of the result are done periodically. A disadvantage of QSs based on a thermal atomic beam is the impossibility of creating compact transportable systems: a thermal atomic beam with an average velocity of atoms of about 500 m s^{-1} is used, and the length of the experimental setup is several meters [46].

A widely used source of atoms in quantum sensoring is currently a MOT of atoms. An atomic fountain can be constructed based on a MOT. Atoms are initially cooled

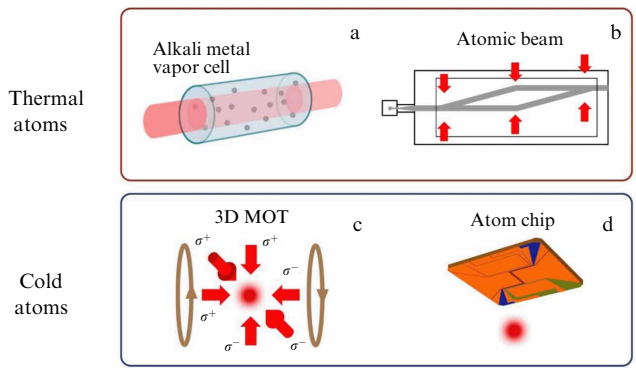

Figure 1. Sources of atoms used to build QSs: (a) alkali metal vapor cell; (b) thermal atomic beam; (c) three-dimensional MOT; (d) atoms trapped near an atom chip.

and trapped in the MOT, with the operating temperatures reaching microkelvins, which allows the atom ensemble to be prepared in the required quantum state with greater accuracy. This ensemble then interacts with physical (magnetic and gravitational) fields. At the end of the interaction stage, the final quantum state of the atomic system is read. The desired parameters of the physical fields are calculated based on the change in this state.

At present, the main application of atomic fountains is in the field of microwave frequency standards [47]. A microwave frequency standard is based on the method of spaced field spectroscopy proposed by Ramsay [48], which is a type of atomic interferometry. The signal detected in a frequency standard depends on the phase difference of two atomic ensembles obtained by coherently splitting the initial ensemble. The phase difference is measured during their recombination. The signal at the output of the atomic interferometer is a set of interference fringes. The sensitivity of such an interferometer is determined by the time between the coherent splitting of the atomic ensemble and its recombination in the detection zone. The width of the interference fringes depends on the width of the velocity distribution of atoms, which is determined by the temperature of the atomic ensemble. Reducing the temperature of atoms in the MOT has allowed achieving a high accuracy in modern frequency standards.

The use of cold atom ensembles formed in a MOT is not limited to frequency standards. At present, gravimeters [23–28], gradiometers [29, 30], gyroscopes [31, 34, 49], and magnetometers [50] based on cold atom ensembles are already being demonstrated. MOTs are sources of atoms not only for laboratory-type atomic interferometers but also for transportable devices [51]. The main research areas are Earth's gravitational field [52] and applications for navigation [53]. Atomic interferometers are also being developed in space on satellites [54, 55] and space stations [56, 57].

Several limitations of using three-dimensional MOTs as atom sources for atomic interferometry can be identified. First, working with a three-dimensional MOT, it is difficult to cool atoms below 1 μK. This temperature is achieved by sub-Doppler cooling methods [58–60]. Achieving lower temperatures with the help of laser fields is a technologically challenging task requiring the use of special cooling methods in cavities [61], Raman cooling [62], and velocity-selective coherent population trapping methods [63]. Yet lower temperatures are usually achieved by evaporative cooling in magnetic or optical traps. The rate of evaporative cooling depends on the concentration of atoms in the trap. In magnetic traps, high concentrations of atoms can be ensured by magnetic compression. This requires high magnetic field gradients, which are difficult to generate using magnetic coils.

Another, no less significant, limitation of the MOT as a source of atoms for QSs is power consumption. The concentration of atoms in a MOT is determined by the magnetic field gradient $B' \sim I_0 N/L^2$ produced by a pair of magnetic coils separated by a distance L and consisting of N turns, with the current I_0 flowing through them. The required current is proportional to the square of the characteristic size of the vacuum chamber, and the power consumption scales as $P \sim L^5$ (assuming that the radius and pitch of the magnetic coils are equal, which is typical of Helmholtz coils). To achieve a gradient of 15 G cm^{-1}, characteristic of the trapping of rubidium atoms, coils consisting of a large number of turns must be used, with a current of the order of several amperes running through them. With the characteristic size of the vacuum chamber determined by the standard vacuum flange of the CF40 standard, the power consumption is then 300 W. With the use of compact systems based on optical cells, which have become popular in recent years, the consumption of MOT coils can be reduced to 5 W [64].

The above limitations are removed when using atom chip technology to provide the magnetic field configuration required for cooling and trapping atoms [65–67]. An atom chip is a solid-state device for creating the magnetic field distribution in three-dimensional space required for cooling, trapping, and controlling neutral atoms. An atom chip allows manipulating the internal and external degrees of freedom of atoms by controlling electric currents flowing through microwires running over its surface. This approach allows the units for cooling, trapping, manipulating, and measuring atomic ensembles to be combined in a single device.

2.1 Advantages of atom chip

The main advantage of atom chips is the possibility of creating high magnetic field gradients. We consider an infinite conductor with a current running through it (Fig. 2). The magnetic field $B(z)$ and the magnetic field gradient $\mathrm{d}B(z)/\mathrm{d}z$ are

$$B(z) = \frac{\mu_0}{2\pi}\frac{I}{z}\,, \tag{1}$$

$$\frac{\mathrm{d}B(z)}{\mathrm{d}z} = -\frac{\mu_0}{2\pi}\frac{I}{z^2}\,, \tag{2}$$

where I is the electric current flowing through the conductor. The magnetic field gradient is inversely proportional to the distance to the conductor squared. Near a current-carrying microwire, a high magnetic field gradient is achieved, which is unattainable when using macroscopic magnetic coils.

To create the magnetic field minimum required for magnetic trapping of atoms, the current-carrying conductor must be placed in an external uniform magnetic field. Such a field can be generated either by external magnetic coils or by additional current-carrying wires. In the latter case, these wires can be placed on the same solid-state substrate as the main conductor. With this configuration, the device can reach the maximum compactness. The distance at which the

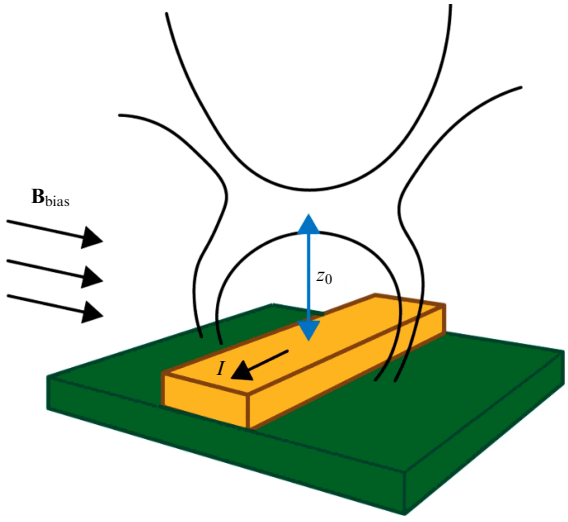

Figure 2. Conductor with current I in uniform magnetic field B_{bias} forms a minimum of the magnetic potential at distance z_0 from atom chip.

magnetic field minimum occurs is

$$z_0 = \frac{\mu_0}{2\pi}\frac{I}{B_{\text{bias}}}, \quad (3)$$

where B_{bias} is the external uniform field in the vicinity of the atom chip.

To form a uniform field in the vicinity of an atom chip, external coils of the Helmholtz configuration are currently used most frequently. A uniform field of a given strength is technically easier to generate than a quadrupole field with a given strength gradient, which is a problem to be solved when creating three-dimensional MOTs. The required current that must run through the magnetic coils to generate a uniform field is proportional to the characteristic dimensions of the device (if a field gradient must be produced, the current is proportional to the square of the characteristic size of the device). For this reason, the electric power consumed by such coils scales as $P \sim L^3$. Consumption of compact devices at the cooling stage is several watts.

The high-gradient magnetic fields allow various applications of atom chips: creation of magnetic atomic waveguides [68, 69], creation of high-density atomic ensembles [70], formation of one-dimensional atomic ensembles [71], and many others. A high magnetic field gradient is indispensable at the evaporative cooling stage. The evaporative cooling rate depends on the atom thermalization time, which in turn depends on the degree of compression of the atomic ensemble. Due to high gradients, this time becomes short, which allows rapid evaporative cooling of atoms to the temperature required to obtain a Bose–Einstein condensate (BEC) [64, 72].

The second advantage of atom chips is their low energy consumption. Indeed, because a high magnetic field gradient is achieved due to the close location of the current-carrying conductor to the atomic ensemble, the current flowing through the conductor can be small. In addition, the spatial dimensions of the conductor are much smaller than the dimensions of the magnetic coils used to create the quadrupole magnetic field of a three-dimensional MOT.

We have noted that a uniform magnetic field is required to form a potential minimum near the atom chip. This field is typically generated by external coils. The QS size is then determined by the size of these magnetic coils. The same applies to the increase in energy consumption of the entire system. However, in comparison with three-dimensional MOTs, a net gain remains, because the important parameter for the use of an atom chip is the magnitude of the magnetic field created by the coils rather than its gradient. The currents running through the coils are codirected and their characteristic values are smaller than in the case where the same coils are used in a three-dimensional MOT configuration, the currents are directed oppositely, and the magnetic field gradient is a relevant factor. As shown at different stages of the experiment with an atom chip [64], using such coils leads to a fivefold gain in energy consumption for rubidium atoms. Moreover, external magnetic coils may be absent altogether, because the required uniform magnetic field can be generated by the current flowing through additional microwires fabricated on the atom chip [73, 74].

The small size and low power consumption allow systems based on atom chips to be used on mobile platforms, including spacecraft. An example is the experiments within the MAIUS [75] and Cold Atom Laboratory [76] programs. In the MAIUS project framework, interference of atoms in a BEC was obtained aboard a rocket in microgravity at an altitude of more than 200 km. In the Cold Atom Laboratory project, experiments with BEC were conducted in microgravity conditions aboard the ISS. In both these examples, the BEC regime is established near the atom chip. These experiments demonstrate a high degree of reliability and technological flexibility of the approaches to controlling atomic ensembles based on atom chip technology. The ongoing merger of the MAIUS and Cold Atom Laboratory projects will allow new experiments to be conducted in microgravity conditions aboard the ISS in the near future [77].

An important parameter of a QS is the number of atoms in the ensemble. It determines the noise limit and hence the accuracy of the QS. It is important to note that the QS compaction achieved using atom chips does not fundamentally affect the number of atoms in a QS. Indeed, in work on creating QSs using three-dimensional MOTs, the number of atoms in an atomic ensemble is about 10^7 [26]. In working with atom chips, it is up to 10^9 atoms [72].

3. Atom chip geometry

Atom chip microwires allow creating different magnetic field distributions near the chip surface. The most common are the so-called U- and Z-shaped configurations [67]. In the U-shaped current configuration, the magnetic field near the atom chip is equivalent to the quadrupole field used in three-dimensional MOTs to produce the primary ensemble of cold atoms. The disadvantage of such a magnetic field distribution is that the magnetic field is zero at the potential minimum in the MOT. The potential minimum allows trapping atoms in the MOT, but does not allow using such a field distribution for magnetic trapping of atoms at the evaporative cooling stage [78]. This problem is solved by using a Z-shaped configuration. In this current configuration, the magnetic field is not zero at the minimum. Reloading of atoms from one type of trap to another is possible by switching electric currents between different wires on the atom chip.

At the first stage of loading into the trap near the atom chip, the atoms are cooled in the U-MOT. The laser field required for cooling the atoms is reflected from the surface of the chip, making up a configuration called the 'mirror' MOT [79]. The quadrupole magnetic field required to form the primary ensemble of cold atoms on the chip is created by the current running through a U-shaped microwire of the atom chip placed in a uniform external magnetic field [79]. This configuration provides a quadrupole magnetic field distribution; the magnetic field is zero at the center of the trap. When shifted off the center, the higher-order multipole (hexapole and octupole) components of the magnetic field become significant, which leads to a deviation of the field distribution from the quadrupole one. The deviation of the magnetic field from being quadrupole makes the capture of atoms less efficient. This, in turn, results in a decrease in the MOT volume where the cooling and trapping of atoms occurs [80].

According to theoretical analysis [81], the number of atoms localized in a MOT is proportional to r^4, where r is the effective radius of the capture region, for a magnetic field assumed to be quadrupole. There are two methods for improving the magnetic field distribution near the atom chip. The first is to use additional wires to compensate for parasitic multipole components of the magnetic field [82, 83]. The advantage of this approach is that no external uniform field is required, and the disadvantage is the need to use high

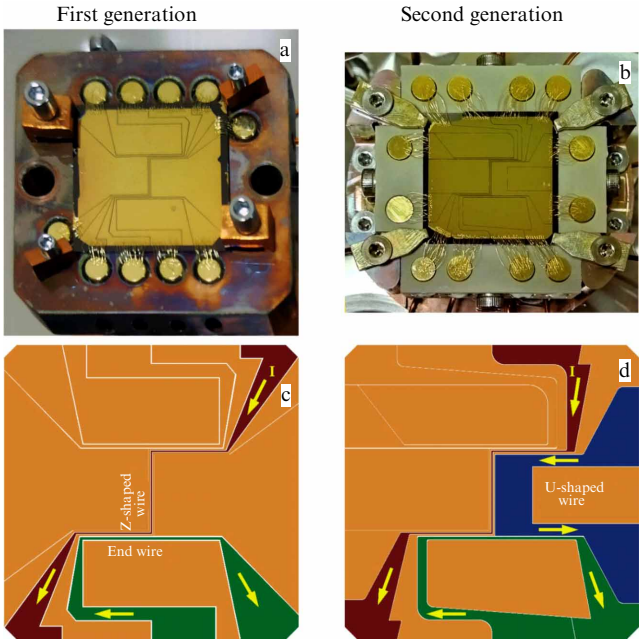

Figure 3. Atom chips of (a) first and (b) second generations created at Institute of Spectroscopy, and (c, d) their outlines.

electric currents, up to 100 A. The second method is to create a U-shaped wire with a wide central part [80, 84]. This approach allows not only obtaining a nearly quadrupole field but also reducing the resistance of the wires, thereby increasing the energy efficiency of the atom chip.

In Fig. 3, we illustrate the concepts of atom chips and show photographs of them. The size of an atom chip is 25×25 mm. At the Institute of Spectroscopy, Russian Academy of Sciences, atom chips were created as follows. A silver-and-gold metal film with a thickness of 5–10 μm was applied to a silicon surface; the microwires of the atom chips were made in the film using lithography. The metal film also serves as a mirror for shaping the MOT. On the first-generation chip, three Z-shaped microwires and two end wires were fabricated. The flow of electric current through a Z-shaped microwire connected to one of the end wires forms a geometry of currents equivalent to a U-shaped microwire. Such a scheme allows localizing the potential minima of the U-MOT and of the magnetic trap at the same spatial point. The reloading of atoms from the MOT into the magnetic trap is effected by switching off the end wire.

The Z-shaped microwires have a width of 100 μm in the region of atom trapping. The end wires are 200 μm wide, which allows several Z-shaped microwires to be used in parallel and one end microwire to distribute the thermal load in the first-generation atom chip [85]. The microwires are spaced by 100 μm.

In the second-generation atom chip, in addition to the above-mentioned microwires, one wide U-shaped microwire with a width of 2.9 mm and a length of 6.2 mm was also manufactured. This allows forming a quadrupole field close to the ideal one in order to increase the number of trapped atoms. From the potential generated by the wide microwire, the atoms are then reloaded into the MOT formed by 'narrow' microwires, with a subsequent reloading of the atoms into the magnetic trap. The reloading of atoms between different MOTs allows a cloud of cold atoms to be compressed, which increases their density.

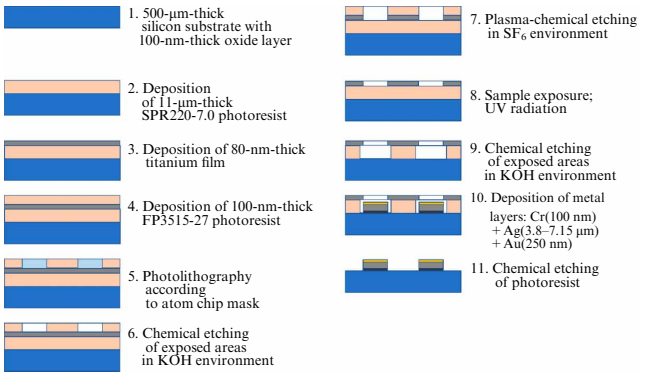

Figure 4. Layout for creating an atom chip based on optical lithography technology.

4. Atom chip fabrication

The atom chip microwires were manufactured using the lift-off lithography method (Fig. 4). A 500-μm-thick, 25×25-mm silicon wafer was used as a substrate. A 100-nm-thick oxide layer was deposited on the wafer to prevent electrical contact between adjacent microwires. In lift-off lithography, the required geometry of the surface structures is defined by a polymer mask, which is removed after the metal film is applied. The next step was atom chip lithography. First, an SPR220-7.0 polymer photoresist, 11 μm in thickness, was applied to the silicon surface. The film was then coated with an 80-nm-thick titanium layer using an electron beam. The titanium film is needed to form a mask required to produce a smooth edge for the future microwires. An FP3515-27 photoresist was applied over the titanium film and was then exposed, with a subsequent removal of the exposed elements by chemical etching in a KOH environment. The exposure was performed using optical lithography. At this stage, the geometry of the atom chip microwires was transferred to the geometry of open titanium nanofilm areas not coated with a photoresist.

The resulting structure was subjected to plasma–chemical etching in an SF_6 atmosphere. This allowed the titanium nanofilm to be removed in those areas where a metal coating had to be applied to the atom chip microwires. Then, the entire chip was exposed to a UV lamp. As a result, the SPR220-7.0 photoresist areas not coated with titanium dissolved in the developer and were removed in the KOH solution. At this stage, a polymer structure coated with a titanium nanofilm forms on the substrate surface. Such structures determine the geometry of gaps between the atom chip microwires. Each polymer strip is covered with a layer of metal, which is necessary for the formation of a smooth edge of the future microwires.

The next stage in fabricating an atom chip is to create a metal microfilm, which is to serve as the atom chip microwires. This is done by thermal spraying of a metal (chrome–silver–gold) film. An important parameter is the level of adhesion of the metal to the dielectric surface. This parameter ensures the future strength of the atom chip. To increase adhesion, a 100-nm chromium layer was deposited. Next, the base metal — silver (3.8 μm for the first-generation and 7.15 μm for the second-generation atom chip) — was applied to the chromium layer, forming a current-carrying wire, onto which an additional 250-nm layer of gold was applied. Gold is a chemically neutral element and exhibits

good reflection in the red part of the spectrum. The process of creating such a three-layer metal film was carried out sequentially under high vacuum conditions. At the final stage, the polymer layer was removed.

5. Cooling and trapping atoms on an atom chip

The use of quantum effects in the functioning of a sensor allows significantly increasing the accuracy of measurements. The ultimate accuracy of a QS is determined by the quantum projection noise (QPN). When using neutral atoms in the sensor, its ultimate accuracy is determined by the number of atoms N in the atomic ensemble of the sensor [86]:

$$\mathrm{QPN} \sim \frac{1}{\sqrt{N}}\,. \tag{4}$$

The number of atoms N in the MOT, in the stationary case, is [87]

$$N = R\tau\,, \tag{5}$$

where R is the rate of loading atoms into the MOT and τ is the lifetime of the atoms in a trap, which is determined by their collisions with residual atoms in the vacuum chamber. In a MOT with a quadrupole magnetic field distribution, the loading rate is typically determined by the area of the laser beams and the flux of atoms. When the field deviates from the quadrupole type, the volume of the domain of effective capture of atoms is determined not by the size of the laser beams but by the size of the domain of small deviations of the magnetic field from the ideal distribution.

To increase the number of atoms localized in a U-shaped MOT near the atom chip, the experimental device parameters must be optimized, including

(1) Optimization of the geometry of the magnetic field distribution near the atom chip;

(2) Increase in the lifetime of atoms in the MOT;

(3) Increase in the flux of atoms entering the trapping region.

Optimization of all these parameters increases the number of trapped atoms. The first condition can be satisfied by choosing the geometry of the atom chip microwire. As calculations show [80, 84, 88], increasing the microwire width along with adding a vertical component of the magnetic field allows making its distribution closer to the quadrupole one.

Increasing the lifetime of atoms on the atom chip is achieved by optimizing the vacuum system, because the lifetime is largely limited by collisions with the buffer gas. To achieve an ultrahigh vacuum in the chamber containing the atom chip, atoms are loaded (using differential pumping) from an atomic beam whose source is located in another part of the vacuum chamber [89].

Increasing the flux of atoms in the atom chip region is also possible by focusing the atoms [90, 91]. We now consider the experimental device and methods of localizing atoms in more detail.

5.1 Experimental device

To build QSs based on cold atoms, the temperature of the atomic ensemble must be kept extremely low. This then allows carrying out measurements with a large base of the atomic interferometer, whose length depends on the velocity of the atoms (the temperature of the atomic ensemble). The interference pattern contrast in the atomic interferometer and hence the sensor sensitivity can be increased by decreasing the temperature and increasing the atomic ensemble density. The maximum atomic ensemble density is achieved when the atoms pass into a BEC.

To increase the trap loading rate while maintaining an ultrahigh vacuum, the atom chip was loaded from an atomic beam. This approach has the following advantages: (1) a local increase in the concentration of atoms while maintaining an ultrahigh vacuum and (2) the possibility of implementing differential pumping. The latter circumstance allows forming an atomic beam in a high-vacuum chamber containing rubidium vapor (saturated or produced by a dispenser) and injecting atoms into the ultrahigh vacuum chamber where the atom chip is located.

Thus, in constructing a QS, the concept underlying the vacuum part of the experimental device for cooling and trapping atoms in the potential created by the atom chip is to use two vacuum chambers: (1) a high-vacuum one, ensuring atomic beam formation, and (2) an ultrahigh-vacuum one for trapping and deep cooling of atoms. Figure 5 shows a photograph and an outline of the experimental device. This device is not intended to illustrate approaches to the compactification of QSs. The main vacuum chamber where the atom chip is located is based on a chamber with a CF160 flange size. On the left is the high-vacuum chamber with a residual vapor pressure of 10^{-8}–10^{-9} Torr and with a rubidium atom dispenser installed. To precool the atoms and increase the atomic beam intensity, precooling is accomplished in this chamber by forming a three-dimensional MOT. A through hole with a diameter of 1 mm is cut in one of the MOT mirrors installed between the high-vacuum precooling chamber and the ultrahigh-vacuum chamber. This hole allows forming an atomic beam of MOT atoms in the differential pumping regime. The hole in the mirror violates the balance of forces in the MOT, which leads to the outflow of atoms from the MOT through the hole into the ultrahigh-vacuum chamber, where the atomic beam is formed. With this method, the atoms typically have an average velocity of about 20 m s^{-1} along the atomic beam, which means that a low-velocity atomic beam is created in the device.

The atomic beam crosses the MOT formed near the atom chip. The transverse size of the atomic beam in the MOT region determines the rate of loading atoms into the MOT. With an atomic beam diameter of about 8 mm, determined by the transverse velocity of atoms and the distance to the atom chip, a large MOT capture area must be provided. This is typically achieved using a mirror MOT consisting of two magnetic coils (shown in gray in the figure) and a laser field, one of whose beams is incident at 45° to the atom chip surface. Near the atom chip, a three-dimensional MOT is formed, similar to that formed in the precooling chamber.

The experimental device is pumped out by turbomolecular and ion-getter pumps. Both sections of the vacuum chamber are provided with magnetic coils for creating the MOT and additional coils for compensating for Earth's magnetic field. Laser radiation is fed into the vacuum chamber using an optical scheme of mirrors and beam splitters. The luminescence signal of atoms is recorded using an sCMOS camera.

The laser part of the experimental device (Fig. 5) consists of two laser radiation sources. The frequency of each is stabilized

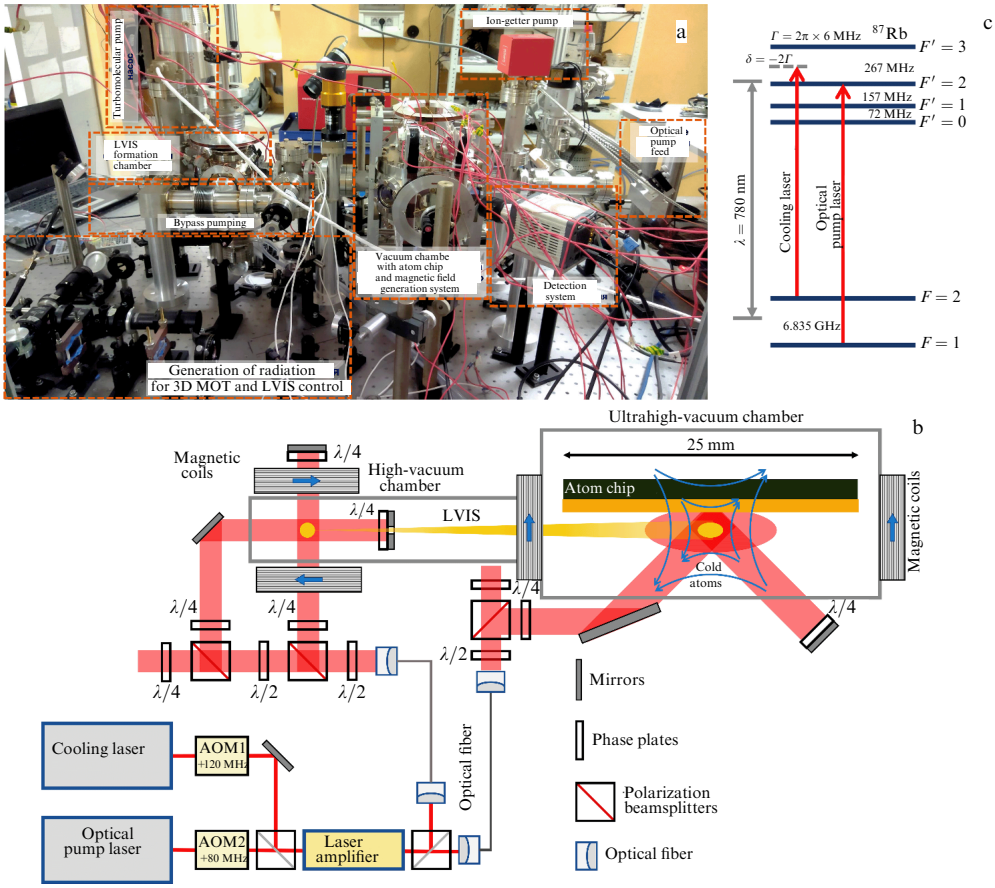

Figure 5. (a) Photograph and (b) schematic diagram of experimental device (not to scale) for laser cooling of atoms and their trapping on an atom chip. (c) Level structure of rubidium-87 atoms.

using a reference cell containing Rb vapor. The main cooling laser is stabilized at the cross resonance $F = 2 \to F' = 2, 3$ of rubidium-87 atoms. The frequency detuning relative to the cyclic transition frequency $F = 2 \to F' = 3$ used for cooling the atoms is 133 MHz. To compensate for such a large detuning and to precisely control it, an acousto-optic modulator (AOM1) with a variable modulation frequency in the range of 50–120 MHz with a two-pass scheme is used. In the stationary atom cooling regime, the AOM1 frequency is set equal to 60 MHz, which corresponds to the detuning of the cooling laser from the exact resonance equal to -13 MHz (-2Γ, where Γ is the width of the resonance absorption line of an atom), which is optimal for cooling the atoms both in the standard and in the U-MOTs on the atom chip. For optical pumping of atoms from the $F = 1$ level of the hyperfine splitting of the ground state to the $F = 2$ level, another laser is used, whose radiation is stabilized at a frequency corresponding to the cross-resonance $F = 1 \to F' = 1, 2$, and is shifted in frequency using the acousto-optic modulator AOM2 to the exact resonance of the $F = 1 \to F' = 2$ transition. The pattern of the rubidium-87 levels used for cooling and the laser frequency positions are shown in Fig. 5.

The number of atoms in the MOT and in the magnetic trap was detected using the fluorescence signal obtained when the atomic ensemble was irradiated by the cooling laser. The laser radiation frequency was chosen the same as at the cooling stage. The pumping laser was also turned on, which allowed the exposure time to be increased. A Hamamatsu Orca sCMOS camera was used to detect the fluorescence signal. The camera was fixed at an angle of 45° to the plane of Fig. 5.

5.2 Atom chip loading

As noted above, we use a low-velocity atomic beam to load atoms into a U-MOT on the atom chip. For this purpose, an experimental device was created consisting of two vacuum chambers with differential pumping: one chamber was for the atomic source with a relatively low vacuum of 10^{-9} Torr, and the other, with a high vacuum of 10^{-10} Torr, was for the atom chip (see Fig. 5). In the first chamber, the atoms were cooled in a three-dimensional MOT, from which a low-velocity atomic beam was then extracted [92]. For this, a through hole (~ 1 mm) was made in the mirror that served to create the laser field configuration required for the three-dimensional MOT. This hole was also an opening for differential pumping. The presence of a hole gives rise to a region free of the laser field in the reflected laser beam, which leads to an imbalance of forces in the central part of the MOT and the appearance of a net force acting on the atoms in the MOT in the direction toward the hole. The atomic beam is directed from the three-dimensional MOT to the chamber containing the atom chip, where further cooling and trapping of the atoms occurs.

On the propagation path of the atomic beam, a region forms where the atoms interact with transverse laser radiation and a two-dimensional quadrupole magnetic field, in order to focus the atomic beam onto the atom chip region [90, 91].

The main idea of focusing atoms using a two-dimensional MOT is as follows [93]. Atoms that have passed through the

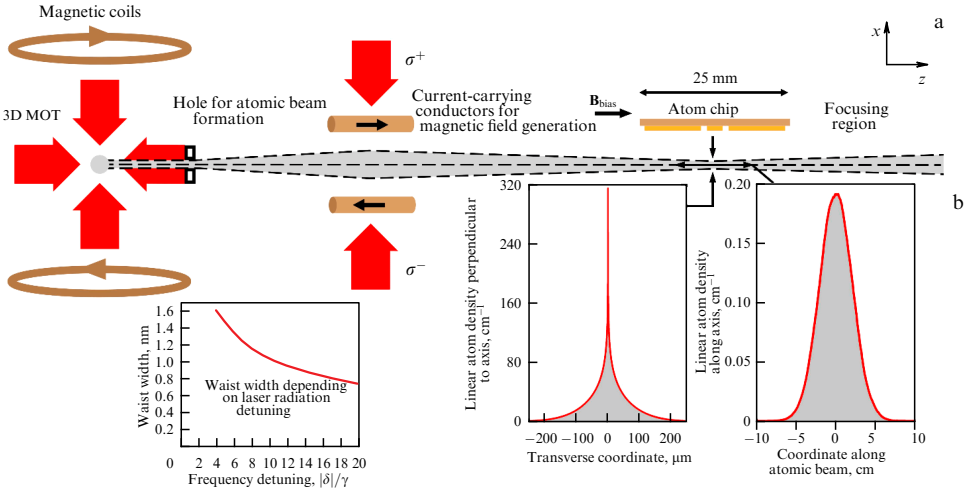

Figure 6. (a) Schematic of focusing atomic beam in the atom chip region, (b) spatial profiles of atomic beam in sub-Doppler and Doppler focusing regimes.

region of the interaction with laser and magnetic fields change their transverse velocity direction due to the light pressure force of the laser field. Because of the magnetic field gradient, the magnitude of this force depends on the transverse coordinate of the atom in the atomic beam. These two factors, under the condition of a sufficiently long residence of atoms in the two-dimensional MOT region, ensure focusing of the atoms such that the focal length of such an atomic lens is independent of the initial transverse velocity of the atoms [94].

Two regimes of focusing by a laser field are possible: (1) the Doppler regime, which is realized at small detunings of the laser field from the exact frequency of the atomic resonance; (2) the sub-Doppler regime, which is realized at large detunings of laser radiation (Fig. 6).

The Doppler focusing regime is characterized by a large value of the atomic momentum diffusion. Given the experimental device parameters, the size of the focusing region was about 8 mm [85].

In the sub-Doppler regime (at large detunings of laser radiation), the momentum diffusion is much smaller, and hence the width of the transverse velocity distribution of atoms during their focusing is smaller. In this regime, the size of the focusing region is about 0.7 mm.

The focusing of the atomic beam results in an increase in the density of atoms in the focal plane. The atom density increases by a factor of 169 compared to the no-focusing case. A further increase in the atom density during focusing can be achieved by decreasing the focal length. When using the sub-Doppler focusing regime, the focal spot size is about 100 μm.

The effect that the interaction of atoms with laser radiation in the intermediate region has on the efficiency of atom loading was studied experimentally in [89]. The setup used allowed spatial scanning of the atomic beam in a plane parallel to the atom chip plane. Figure 7 shows the time dependences of the number of atoms in the MOT formed on the atom chip. The time is referenced to switching on the laser field that generates the atomic beam and ensures cooling on the atom chip.

Comparisons were made of the loading rates of the atom chip from vapors and from an atomic beam. When loading atoms from atomic vapor, the number of atoms in the MOT is an order of magnitude smaller. This is explained by the short

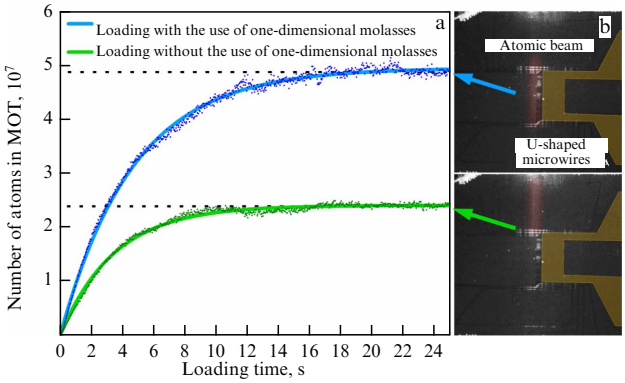

Figure 7. (a) Dynamics of MOT loading from atomic beam near an atom chip without (green curve) and with (blue curve) correction of the spatial position. (b) Photograph of atom chip with spatial position of atomic beam highlighted in red in both cases.

lifetime of atoms in the MOT, which is limited by the pressure of residual vapor in the vacuum chamber. Loading atoms from a low-velocity atomic beam allowed increasing the number of atoms localized in the MOT. The loading dynamics and the number of atoms in the stationary state depend on the position of the atomic beam, which is controlled by the interaction of atoms with a one-dimensional optical molasses. The optimal position is when the atomic beam passes through the central part of the atom chip (blue curve). Figure 7 shows an image of the atomic beam on the background of the atom chip, demonstrating its spatial position (the atomic beam propagates from left to right; the probe laser beam propagates from top to bottom; their intersection is shown in red). It can be seen that, when the atomic beam is shifted relative to the U-shaped microwire, the number of atoms in the MOT decreases (green curve).

5.3 Mirror magneto-optical trap

An important stage in the formation of an atomic ensemble on an atom chip is the cooling of atoms. Currently, the most effective method for obtaining an ensemble of cold atoms is to use a MOT, which allows both cooling and spatially localizing the atoms. The concentration of atoms in a MOT reaches 10^{10} cm^{-3} at a temperature of about 100 μK. Using sub-Doppler cooling methods, the temperature can be

reduced to a few microkelvin. When using a three-dimensional MOT, thermal atoms entering the area of the six laser-beam intersection experience a force directed against their motion, which is analogous to friction force. At less-than-critical initial velocities, atoms are cooled to a temperature corresponding to the Doppler limit ($T_D = 145$ μK for Rb atoms). In addition to laser radiation, a quadrupole magnetic field is present in the cooling area, and therefore the atoms feel the effect of an additional force directed toward the center of the trap, where the quadrupole magnetic field is zero. Under this interaction, the atoms are cooled and trapped in the three-dimensional MOT.

In an atom chip, the atoms are cooled and trapped in a U-MOT formed by the magnetic field of the chip, equivalent to a quadrupole magnetic field. This trap is analogous to the classical three-dimensional MOT. However, the presence of the atom chip makes six independent laser beams impossible to arrange. In this case, a mirror MOT configuration is used [79], where the laser field is due to two laser beams propagating toward each other and parallel to the atom chip surface and due to two other beams that propagate at an angle to the atom chip surface and, having reflected from the surface, make up a laser field functionally equivalent to the laser field of a traditional three-dimensional MOT.

To create the required magnetic field, the current $I_0 = 3$ to 10 A, depending on the microwires used, must flow through the atom chip microwires. In the second-generation atom chip, the primary U-MOT is formed when the current flows through a 'wide' microwire. The 'wide' microwire allows using a current of up to 10 A without significant heating of the atom chip. At the same time, the large width of the U-shaped wire allows creating a magnetic field distribution close to the quadrupole one [80, 84, 88]. The atoms can then be reloaded into the U-MOT formed by 'narrow' wires. This stage is necessary for compressing the atomic cloud and increasing the concentration of atoms for their further reloading into the magnetic trap.

In accordance with expressions (1)–(3), a large current through the 'wide' U-shaped microwires allows a minimum of the quadrupole field to be attained at a macroscopic distance (3 mm) from the atom chip upon reaching the required magnetic field gradient (about 15 G cm^{-1}). The minimum of the magnetic field was arranged using an external uniform field of 5 G directed parallel to the atom chip plane and a magnetic field of 2.1 G in the perpendicular direction. The number of atoms localized in this trap was 50×10^6. The same number of atoms is cooled in the atomic ensemble, which plays the role of a gravimeter in the QS when using a pyramidal MOT [26]. At the stage of reloading of atoms between traps, the electric current flowing through the 'wide' microwire is switched off. At the same time, a 3-A current through the 'narrow' Z-shaped microwire and the end wire is switched on, which gives rise to a minimum of the quadrupole field at a distance of 1.2 mm from the atom chip. The external uniform field directed along the atom chip then has a magnitude of 3.5 G, and the vertical component, 1.6 G. Reloading takes about 10 ms, with a 95% efficiency.

The primary atomic ensemble is a source of atoms for the next atom trap, which has a smaller volume. Figure 8 shows images of atoms before and after reloading, obtained by recording the fluorescence of atoms excited by a laser field. The magnitude of the fluorescence signal is proportional to the number of atoms in the trap, which allows measuring the lifetime of atoms in the MOT; it was found to be 4.1 s [89]. The method of measuring the lifetime of atoms near the atom chip can be used to construct precision vacuum gauges [17].

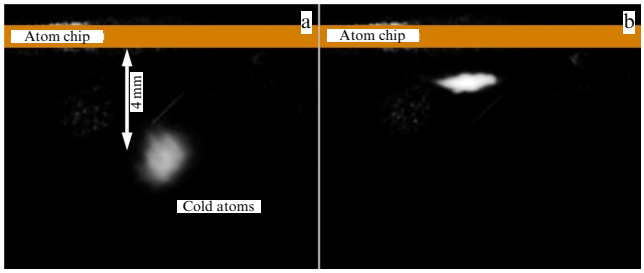

Figure 8. Images of a cloud of cold atoms trapped in a (a) 'wide' and (b) 'narrow' U-MOT, obtained by detecting fluorescence of atoms under their laser excitation.

5.4 Trapping of atoms in magnetic potential

After the atoms are reloaded into the 'narrow' U-MOT, their magnetic localization can be ensured. For this, the magnetic field distribution must be changed from the quadrupole to the Ioffe–Pritchard trap distribution. The latter is formed by a Z-shaped microwire placed in a uniform magnetic field. Because the field in the 'narrow' U-MOT is created by the Z-shaped and end microwires (see Fig. 3), it suffices to switch off the end microwire to form the spatial distribution of the Ioffe–Pritchard magnetic field. With this approach, the MOT and the magnetic trap are spatially superimposed, which facilitates reloading the atoms from one trap to another. However, with the described procedure for loading atoms into the magnetic trap, the number of atoms localized in the magnetic trap is small. This is due to two factors. First, the temperature of the atomic ensemble in the MOT corresponds to the Doppler limit and is about 145 μK. Second, only atoms located at certain magnetic sublevels are localized in the magnetic trap. In the case of rubidium-87, such sublevels of the ground state are $|F = 1, m_F = -1\rangle$ and $|F = 2, m_F = 1$ and $2\rangle$. Because the atoms in the MOT are distributed over different magnetic sublevels, not all atoms are trapped.

To increase the number of atoms in the magnetic trap, those in the 'narrow' U-MOT were subjected to sub-Doppler cooling. For this, the cooling radiation frequency was changed from $\delta = -2\Gamma$ to $\delta = -4.2\Gamma$. Sub-Doppler cooling was followed by the optical pumping of atoms to the magnetic sublevel of the ground state that allows localizing atoms in the magnetic trap. At the optical pumping stage, the current through all the wires of the atom chip is completely switched off. Only the external uniform bias field remains, which serves to determine the quantization axis. The optical pumping time is 1 ms.

Next, the current through the wires of the atom chip is switched on, which creates the magnetic trap potential; subsequently, the external uniform magnetic field is increased in order to increase the magnetic potential depth. In the experiment, about 2% of the initial number of atoms cooled at the wide U-MOT stage were localized in the magnetic trap.

Figure 9 shows the time dependence of the number of atoms in the magnetic trap, whence the lifetime of atoms in the trap was determined. The dots show the experimentally measured number of atoms in the magnetic trap depending on the confinement time. This dependence was approximated by

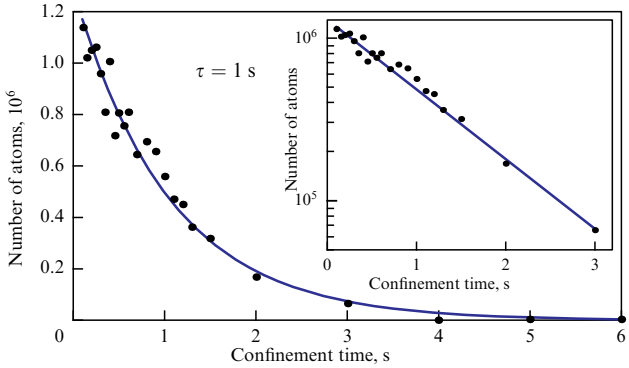

Figure 9. Dependence of the number of atoms in a magnetic trap on time. Inset shows same graph on a logarithmic scale.

an exponential with a characteristic lifetime $\tau = 1$ s. This type of lifetime dependence is typical of the interaction of trapped atoms and the residual buffer gas.

6. Conclusion

The use of atom chips to cool and trap cold atoms offers a number of advantages. The main one is the ability to create high magnetic field gradients near the atom chip surface. This allows the formation of ensembles of ultracold atoms with a temperature of less than 1 μK in a minimum time, which is challenging when using other cooling methods. In addition, atom chips allow a high degree of compactness to be achieved and in the future will make it possible to produce compact devices [65].

The main disadvantages of atom chips include the need for additional magnetic coils and atom precooling systems. The presence of coils sets a limit on the compactness of QSs. Importantly, however, the use of external coils to create a uniform magnetic field in the atom chip region is much simpler compared with the case of coils that create a magnetic field gradient for cooling atoms in a three-dimensional MOT. An additional stage of atom cooling and differential pumping is inherent in all systems using ultracold atoms. It is indispensable because of the need for an ultrahigh vacuum in the atom chip region when forming an atomic ensemble in the BEC state. Currently, approaches to loading atom chips from vapor produced in the same vacuum chamber where the atom chip is located are being considered [95]. However, this method limits the lifetime of atoms in the magnetic trap. The precooling system can be abandoned when using an atom chip as a source of atoms with a temperature above 1 μK without their localization in a magnetic trap. Currently, the presence of an additional chamber for differential pumping and shaping a precooled atomic beam is not a limitation on the size of QSs. The main limitation is the size of the magnetic shields that are necessary in any sensor based on cold atoms to screen Earth's magnetic field and that of nearby devices. Such shielding is necessary for the operation of atomic interferometers, namely, for the subsequent setting of the quantization axis with additional coils being included. If magnetic shields were absent, the quantization axis direction would fluctuate, leading to additional noise.

Having compared various methods of trapping of atoms, we can say that the use of an atom chip is not inferior to other methods. For comparison, a three-dimensional MOT can allow trapping up to 10^9 atoms at a concentration of about 10^{10} cm^{-3} [87]. This can be achieved by exposure to laser beams over a large area. With the use of dipole traps, which do not require a magnetic field, a higher density of atoms can be achieved, up to 10^{13} cm^{-3}, with 10^7 atoms [96]. Three-dimensional magnetic traps allow localizing up to 10^9 atoms with a concentration of about 10^{11} cm^{-3} [97]. Methods that do not rely on magnetic fields for cooling and trapping atoms allow capturing up to 10^7 atoms [98]. A comparison makes it clear that trapping of atoms near the atom chip is a tool that is not inferior to other methods capable of localizing up to 10^9 atoms at the MOT stage and 10^8 in a magnetic trap [72]. The choice of one method or another is determined by the ultimate goal.

The main advantage of atom chip technology over other methods is the possibility of rapid evaporative cooling to temperatures below 1 μK. Evaporative cooling can also be implemented in optical traps. In that case, the requirement that atoms be in a quantum state with a particular projection of the magnetic moment onto the quantization axis is dropped. It becomes possible to use Feshbach resonances to control the interaction of atoms in the trap [99]. From the standpoint of constructing a QS, the use of an additional laser radiation source would lead to a more complex optical part of the sensor. On the other hand, evaporative cooling near the atom chip is achieved by monitoring electric currents running through the microwires. This method does not require additional optical elements and their alignment, and monitoring electric currents is easier to implement from the technological standpoint.

Over the past decade, quantum technologies based on atom chips have become a powerful platform for scalable atomic quantum-optical systems with various applications. Numerous configurations of atom chips have been developed that allow cooling and trapping ultracold atoms and degenerate BECs near the chip surface, with their internal and external degrees of freedom effectively controlled for quantum sensoring and metrology tasks. One of the development avenues is the unification of atom and optical chips [100]. Also important is to expand the range of atom species that can be cooled and localized on an atom chip [101].

The greatest progress in developing QSs has been achieved in fundamental areas. Among the fundamental problems that can be solved using QSs based on neutral atoms, the following can be highlighted: detection of gravitational waves [102], search for dark matter [103], study of coupling to dark energy [104], and tests of the equivalence principle [105] and of the validity of quantum mechanics on a macroscopic scale [106]. All of these areas require precision control of atomic ensembles. The most accurate experiments are planned to be carried out aboard spacecraft [51]. From this standpoint, atom chips are the most popular platform for creating compact and energy-efficient QSs.

This study was supported by the Russian Science Foundation, grant no. 23-22-00255.

References

1. Degen C L, Reinhard F, Cappellaro P *Rev. Mod. Phys.* **89** 035002 (2017)
2. Balykin V I, Minogin V G, Letokhov V S *Rep. Prog. Phys.* **63** 1429 (2000)
3. Balykin V I *Phys. Usp.* **54** 844 (2011); *Usp. Fiz. Nauk* **181** 875 (2011)
4. Phillips W D *Rev. Mod. Phys.* **70** 721 (1998); *Usp. Fiz. Nauk* **169** 305 (1999)

5. Cornell E A, Wieman C E *Rev. Mod. Phys.* **74** 875 (2002); *Usp. Fiz. Nauk* **173** 1320 (2003)
6. DeMarco B, Jin D S *Science* **285** 1703 (1999)
7. O'Hara K M et al. *Science* **298** 2179 (2002)
8. Onofrio R *Phys. Usp.* **59** 1129 (2016); *Usp. Fiz. Nauk* **186** 1229 (2016)
9. Barmashova T V et al. *Phys. Usp.* **59** 174 (2016); *Usp. Fiz. Nauk* **186** 183 (2016)
10. Nicholson T L et al. *Nat. Commun.* **6** 1 (2015)
11. Taichenachev A V, Yudin V I, Bagayev S N *Phys. Usp.* **59** 168 (2016); *Usp. Fiz. Nauk* **186** 193 (2016)
12. Graham T M et al. *Nature* **604** 457 (2022)
13. Georgescu I M, Ashhab S, Nori F *Rev. Mod. Phys.* **86** 153 (2014)
14. Vishnyakova G A et al. *Phys. Usp.* **59** 168 (2016); *Usp. Fiz. Nauk* **186** 176 (2016)
15. Makhalov V B, Martiyanov K A, Turlapov A V *Metrologia* **53** 1287 (2016)
16. Makhalov V B, Turlapov A V *Quantum Electron.* **47** 431 (2017); *Kvantovaya Elektron.* **47** 431 (2017)
17. Supakar S et al. *J. Appl. Phys.* **134** (2023)
18. Zheng X et al. *Nat. Commun.* **14** 4886 (2023)
19. Grotti J et al. *Nature Phys.* **14** 437 (2018)
20. Takamoto M et al. *Nat. Photon.* **14** 411 (2020)
21. Barontini G et al. *EPJ Quantum Technol.* **9** 12 (2022)
22. Bongs K et al. *Nat. Rev. Phys.* **1** 731 (2019)
23. Altin P A et al. *New J. Phys.* **15** 023009 (2013)
24. Hu Z-K et al. *Phys. Rev. A* **88** 043610 (2013)
25. Huang P-W et al. *Metrologia* **56** 045012 (2019)
26. Ménoret V et al. *Sci. Rep.* **8** 12300 (2018)
27. Li D et al. *Sensors* **23** 5089 (2023)
28. Ge G et al. *Sensors* **23** 6115 (2023)
29. Sorrentino F et al. *Phys. Rev. A* **89** 023607 (2014)
30. Stray B et al. *Nature* **602** 590 (2022)
31. Durfee D S, Shaham Y K, Kasevich M A *Phys. Rev. Lett.* **97** 240801 (2006)
32. Dubetsky B, Kasevich M A *Phys. Rev. A* **74** 023615 (2006)
33. Wu S, Su E, Prentiss M *Phys. Rev. Lett.* **99** 173201 (2007)
34. Gauguet A et al. *Phys. Rev. A* **80** 063604 (2009)
35. Geiger R et al. *AVS Quantum Sci.* **2** 024702 (2020)
36. Fortágh J, Zimmermann C *Rev. Mod. Phys.* **79** 235 (2007)
37. Budker D, Jackson Kimball D F (Eds) *Optical Magnetometry* (Cambridge: Cambridge Univ. Press, 2013)
38. Makarov A O, Brazhnikov D V, Goncharov A N *JETP Lett.* **117** 509 (2023); *Pis'ma Zh. Eksp. Teor. Fiz.* **117** 509 (2023)
39. Vanier J *Appl. Phys. B* **81** 421 (2005)
40. Chuchelov D S et al. *JETP Lett.* **119** 16 (2024); *Pis'ma Zh. Eksp. Teor. Fiz.* **119** 16 (2024)
41. Keith D W et al. *Phys. Rev. Lett.* **61** 1580 (1988)
42. Balykin V I, Letokhov V S, Sidorov A I *JETP Lett.* **40** 1026 (1984); *Pis'ma Zh. Eksp. Teor. Fiz.* **40** 251 (1984)
43. Lett P D et al. *J. Opt. Soc. Am. B* **6** 2084 (1989)
44. Moskowitz P E et al. *Phys. Rev. Lett.* **51** 370 (1983)
45. Gustavson T L, Bouyer P, Kasevich M A *Phys. Rev. Lett.* **78** 2046 (1997)
46. Gustavson T L, Landragin A, Kasevich M A *Class. Quantum Grav.* **17** 2385 (2000)
47. Wynands R, Weyers S *Metrologia* **42** S64 (2005)
48. Ramsey N F *Phys. Rev.* **78** 695 (1950)
49. Feng D *IOP Conf. Ser. Earth Environ. Sci.* **237** 032027 (2019)
50. Eto Y et al. *Phys. Rev. A* **88** 031602 (2013)
51. Geiger R et al., arXiv:2003.12516
52. Bidel Y et al. *Nat. Commun.* **9** 627 (2018)
53. Barrett B, Bertoldi A, Bouyer P *Phys. Scr.* **91** 053006 (2016)
54. Liu L et al. *Nat. Commun.* **9** 2760 (2018)
55. Devani D et al. *CEAS Space J.* **12** 539 (2020)
56. Ren W et al. *Natl. Sci. Rev.* **7** 1828 (2020)
57. Li H et al. *Chinese Opt. Lett.* **21** 080201 (2023)
58. Salomon C et al. *Europhys. Lett.* **12** 683 (1990)
59. Dalibard J, Cohen-Tannoudji C *J. Opt. Soc. Am. B* **6** 2023 (1989)
60. Chang S et al. *Phys. Rev. A* **60** 3148 (1999)
61. Wolke M et al. *Science* **337** 75 (2012)
62. Davidson N et al. *Phys. Rev. Lett.* **72** 3158 (1994)
63. Hack J et al. *Phys. Rev. A* **62** 013405 (2000)
64. Farkas D M, Salim E A, Ramirez-Serrano J, arXiv:1403.4641
65. Keil M et al. *J. Mod. Opt.* **63** 1840 (2016)
66. Reichel J, Vuletić V (Eds) *Atom Chips* (Weinheim: Wiley-VCH Verlag, 2011)
67. Reichel J *Appl. Phys. B* **74** 469 (2002)
68. Reichel J et al. *Appl. Phys. B* **72** 81 (2001)
69. Cassettari D et al. *Appl. Phys. B* **70** 721 (2000)
70. Horikoshi M, Nakagawa K *Appl. Phys. B* **82** 363 (2006)
71. van Amerongen A H et al. *Phys. Rev. Lett.* **100** 090402 (2008)
72. Rudolph J et al. *New J. Phys.* **17** 065001 (2015)
73. Thywissen J H et al. *Eur. Phys. J. D* **7** 361 (1999)
74. Dekker N H et al. *Phys. Rev. Lett.* **84** 1124 (2000)
75. Becker D et al. *Nature* **562** 391 (2018)
76. Aveline D C et al. *Nature* **582** 193 (2020)
77. Frye K et al. *EPJ Quantum Technol.* **8** 1 (2021)
78. Ott H et al. *Phys. Rev. Lett.* **87** 230401 (2001)
79. Reichel J, Hänsel W, Hänsch T W *Phys. Rev. Lett.* **83** 3398 (1999)
80. Wildermuth S et al. *Phys. Rev. A* **69** 030901 (2004)
81. Monroe C et al. *Phys. Rev. Lett.* **65** 1571 (1990)
82. Jöllenbeck S et al. *Phys. Rev. A* **83** 043406 (2011)
83. Hyodo M et al. *Phys. Rev. A* **76** 013419 (2007)
84. Singh V et al. *J. Mod. Opt.* **65** 2332 (2018)
85. Afanasiev A E et al. *Opt. Laser Technol.* **148** 107698 (2022)
86. Santarelli G et al. *Phys. Rev. Lett.* **82** 4619 (1999)
87. Steane A M, Chowdhury M, Foot C J *J. Opt. Soc. Am. B* **9** 2142 (1992)
88. Skakunenko P et al. *Chinese Opt. Lett.* **22** 060201 (2024)
89. Skakunenko P I et al. *JETP Lett.* **119** 20 (2024); *Pis'ma Zh. Eksp. Teor. Fiz.* **119** 20 (2024)
90. Afanasiev A E et al. *JETP Lett.* **115** 509 (2022); *Pis'ma Zh. Eksp. Teor. Fiz.* **115** 562 (2022)
91. Bykova D V, Afanasiev A E, Balykin V I *JETP Lett.* **118** 14 (2023); *Pis'ma Zh. Eksp. Teor. Fiz.* **118** 7 (2023)
92. Lu Z T et al. *Phys. Rev. Lett.* **77** 3331 (1996)
93. Balykin V I *JETP Lett.* **66** 349 (1997); *Pis'ma Zh. Eksp. Teor. Fiz.* **66** 327 (1997)
94. Melentiev P N et al. *JETP Lett.* **83** 14 (2006); *Pis'ma Zh. Eksp. Teor. Fiz.* **83** 16 (2006)
95. Singh V et al. *J. Appl. Phys.* **133** 084402 (2023)
96. Grimm R, Weidemüller M, Ovchinnikov Yu B *Adv. Atom. Mol. Opt. Phys.* **42** 95 (2000)
97. Moore K L et al. *Appl. Phys. B* **82** 533 (2006)
98. Prudnikov O N et al. *Phys. Rev. A* **108** 043107 (2023)
99. Davletov E T et al. *Phys. Rev. A* **102** 011302 (2020)
100. Chen L et al. *Phys. Rev. Applied* **17** 034031 (2022)
101. Vyalykh A P et al. *JETP Lett.* **119** 285 (2024); *Pis'ma Zh. Eksp. Teor. Fiz.* **119** 273 (2024)
102. Hogan J M, Kasevich M A *Phys. Rev. A* **94** 033632 (2016)
103. Arvanitaki A et al. *Phys. Rev. D* **97** 075020 (2018)
104. Jaffe M et al. *Nature Phys.* **13** 938 (2017)
105. Rosi G et al. *Nat. Commun.* **8** 15529 (2017)
106. Kovachy T et al. *Nature* **528** 530 (2015)